The Signature of the Annular Modes in the Tropical Troposphere

DAVID W. J. THOMPSON

Department of Atmospheric Science, Colorado State University, Fort Collins, Colorado

DAVID J. LORENZ

Department of Atmospheric Sciences, University of Washington, Seattle, Washington

(Manuscript received 23 June 2003, in final form 13 April 2004)

ABSTRACT

The extratropical annular modes are coupled with a distinct pattern of climate anomalies that spans the circulation of the tropical troposphere. The signature of the annular modes in the tropical troposphere exhibits a high degree of equatorial symmetry. It is associated with upper-tropospheric zonal wind anomalies centered about the equator, midtropospheric temperature anomalies located ~20°N and 20°S, and opposing mean meridional circulation anomalies that span the subtropics of both hemispheres. The linkages between the annular modes and the tropical circulation are only evident during the cold season months, and are most robust in association with the Northern Hemisphere annular mode (NAM).

The coupling between the annular modes and the circulation of the tropical troposphere is consistent with forcing by waves originating at extratropical latitudes. Both annular modes are characterized by anomalies in the eddy momentum flux convergence at tropical latitudes that act to reinforce the changes in the tropical wind and temperature fields. The most pronounced tropical anomalies lag indices of the annular modes by ~2 weeks and are found over the eastern tropical Pacific, where climatological westerlies permit extratropical waves to propagate into the deep Tropics. The linkages between the NAM and the tropical tropospheric circulation are most pronounced during the cold phase of the El Niño–Southern Oscillation cycle.

The recent trend in the NAM is linearly congruent with a ~0.1-K cooling of the tropical troposphere over the past two decades during the Northern Hemisphere winter season.

1. Introduction

The Northern and Southern Hemisphere annular modes dominate large-scale climate variability in their respective hemispheres. The structure of the Northern Hemisphere annular mode (NAM) is discussed in, for example, Walker and Bliss (1932), van Loon and Rogers (1978), Wallace and Gutzler (1981), Hurrell (1995), and Thompson and Wallace (1998, 2000); the structure of the Southern Hemisphere annular mode (SAM) is shown in Rogers and van Loon (1982), Mo and White (1985), Yoden et al. (1987), Kidson (1988a,b), Karoly (1990), Shiotani (1991), Hartmann and Lo (1998), and Thompson and Wallace (2000). Both annular modes are associated with equivalent barotropic vacillations in the strength of the zonal flow between centers of action located at ~35°–40° and ~55°–60° latitude. Periods when the zonal flow along ~55°–60° latitude is anomalously westerly (the so-called high index polarity of the annular modes) are characterized by lower-than-normal geopotential heights and temperatures over the polar cap, and by higher-than-normal geopotential heights and temperatures in the midlatitudes centered at ~45°. The NAM is alternatively referred to as the North Atlantic Oscillation (Hurrell et al. 2002) and the Arctic Oscillation (Thompson and Wallace 1998); the SAM is alternatively referred to as the High-Latitude Mode (Karoly 1990) and the Antarctic Oscillation (Gong and Wang 1999; Thompson and Wallace 2000).

The annular modes owe their existence to wave–mean flow interactions in the extratropical circulation (e.g., Karoly 1990; Hartmann and Lo 1998; Thompson and Wallace 2000; Limpasuvan and Hartmann 1999, 2000; Lorenz and Hartmann 2001, 2003). During their high index polarity, anomalous poleward eddy momentum fluxes in the upper troposphere at ~45° latitude give rise to anomalous convergence of the eddy momentum flux and westerly wind anomalies along ~55°–60° latitude, and to anomalous divergence of the eddy momentum flux and easterly wind anomalies along ~35°–40° latitude. In turn, the zonal wind anomalies associated with the annular modes organize eddy activity such that the resulting eddy momentum flux anomalies reinforce the anomalies in the zonal flow (Robinson 2000;

Corresponding author address: Dr. David W. Thompson, Dept. of Atmospheric Science, Colorado State University, Fort Collins, CO 80523-1371.
E-mail: davet@atmos.colostate.edu

Lorenz and Hartmann 2001, 2003). The resulting positive feedback between the zonal flow and the eddies acts to enhance the variability of the annular modes relative to the background spectrum of climate variability, and it helps account for the selection of the annular modes as the leading patterns of variability in their respective hemispheres (Lorenz and Hartmann 2001, 2003).

The annular modes have largest amplitude at extratropical latitudes, but several studies reveal that they have a substantial signature at tropical latitudes as well. Most of these studies focus on regional relationships between the NAM and tropical variability over the Atlantic sector. For example, Meehl and van Loon (1979) show that the NAM is significantly correlated with the strength of the trade winds over the North Atlantic and with the position of the intertropical convergence zone over Africa, Lamb and Peppler (1987) note that the NAM has a significant signature in Moroccan rainfall, Moulin et al. (1997) demonstrate that the NAM is linked to anomalous dust transport from the Sahara desert, Malmgren et al. (1998) show that the NAM is reflected in Puerto Rican rainfall, McHugh and Rogers (2001) demonstrate that the NAM is coupled with variations in eastern African rainfall, and Czaja et al. (2002) show that the NAM accounts for a substantial fraction of tropical Atlantic sea surface temperature variability. Thompson and Wallace (2000) demonstrate that the annular modes are characterized by fluctuations in the strength of the trade winds throughout the subtropics of their respective hemispheres, and Baldwin (2001) notes that both annular modes are associated with variations in sea level pressure that extend into the deep Tropics.

In this study, we examine the signature of the annular modes in the tropical troposphere in greater detail. It is shown that both annular modes are associated with variations in the tropospheric circulation that not only transcend the extratropics of their respective hemispheres, but that span the circulation of the Tropics and extend into the subtropics of the opposing hemisphere as well. The paper is divided into four subsequent sections. In section 2, we discuss the data and methodology used in the analysis. Section 3 demonstrates that the NAM is coupled with a distinctive pattern of tropical tropospheric circulation anomalies that lags variations in the NAM by roughly 2 weeks. It is hypothesized that the tropical features of the NAM are consistent with forcing by waves originating at extratropical latitudes. Section 3 also demonstrates that the amplitude of the tropical signature of the NAM is a function of the phase of the El Niño–Southern Oscillation (ENSO) cycle. Section 4 examines analogous features observed in association with the SAM, and section 5 offers a synthesis and discussion of the results.

2. Data and methodology

The primary data used in this study are the 4 times daily fields of the National Centers for Environmental Prediction–National Center for Atmospheric Research (NCEP–NCAR) reanalysis from 1979 to 1999 (Kalnay et al. 1996), obtained from the National Oceanographic and Atmospheric Administration (NOAA) Climate Diagnostics Center (CDC). Data following the incorporation of satellite data in the reanalysis in 1979 are considered most reliable for the purpose of this study. Results are also presented for Microwave Sounding Unit channel 2LT temperature data (MSU2LT; Spencer and Christy 1992) and for surface temperature data described in Jones (1994).

Temporal variability in the annular modes is defined on the basis of the standardized leading principal component time series of daily mean sea level pressure (Northern Hemisphere) and 850-hPa geopotential height (Southern Hemisphere) anomalies calculated for the domain of 20°–90° latitude. Daily time series of the NAM and the SAM are available online via the NOAA Climate Prediction Center (http://www.cpc.ncep.noaa.gov). By convention, the high index polarity of the annular modes is defined as stronger than normal westerlies along ~55°–60° latitude, and vice versa.

The statistical significance of all correlation coefficients is assessed using the *t* statistic. The effective sample size is estimated using the relationship outlined in Bretherton et al. (1999), which applies when testing the significance of second-order moments of time series:

$$N_{\text{eff}} = N\left(\frac{1 - r_1 r_2}{1 + r_1 r_2}\right), \tag{1}$$

where N_{eff} is the effective sample size; N is the sample size; and r_1 and r_2 are the lag-1 autocorrelations of the time series being correlated. For example, in the case of the daily annular mode indices and for $r_1 \cong r_2$, the ratio $N_{\text{eff}}/N \cong 0.05$, which corresponds to ~1 degree of freedom 20 days^{-1}.

Variations in the ENSO cycle are defined on the basis of sea surface temperature anomalies averaged between 6°N–6°S and 180°–90°W, hereafter referred to as the cold tongue index (CTI) time series. The CTI time series used in this study is available online at the Joint Institute for the Study of the Atmosphere and the Oceans at the University of Washington (online at http://jisao.washington.edu).

3. The signature of the NAM in the tropical troposphere

The signature of the NAM in the tropical troposphere is examined in daily averaged data centered on the winter season months January–March (JFM). In cases where we calculate lagged regression coefficients, the calendar dates used in the analysis extend from December to April. For example, when the regression is lagged by 2 weeks, the predictor is based on 1 January–31 March, and the predictand on 15 January–14 April. The relationships between the NAM and the tropical troposphere revealed in this section were found to be most

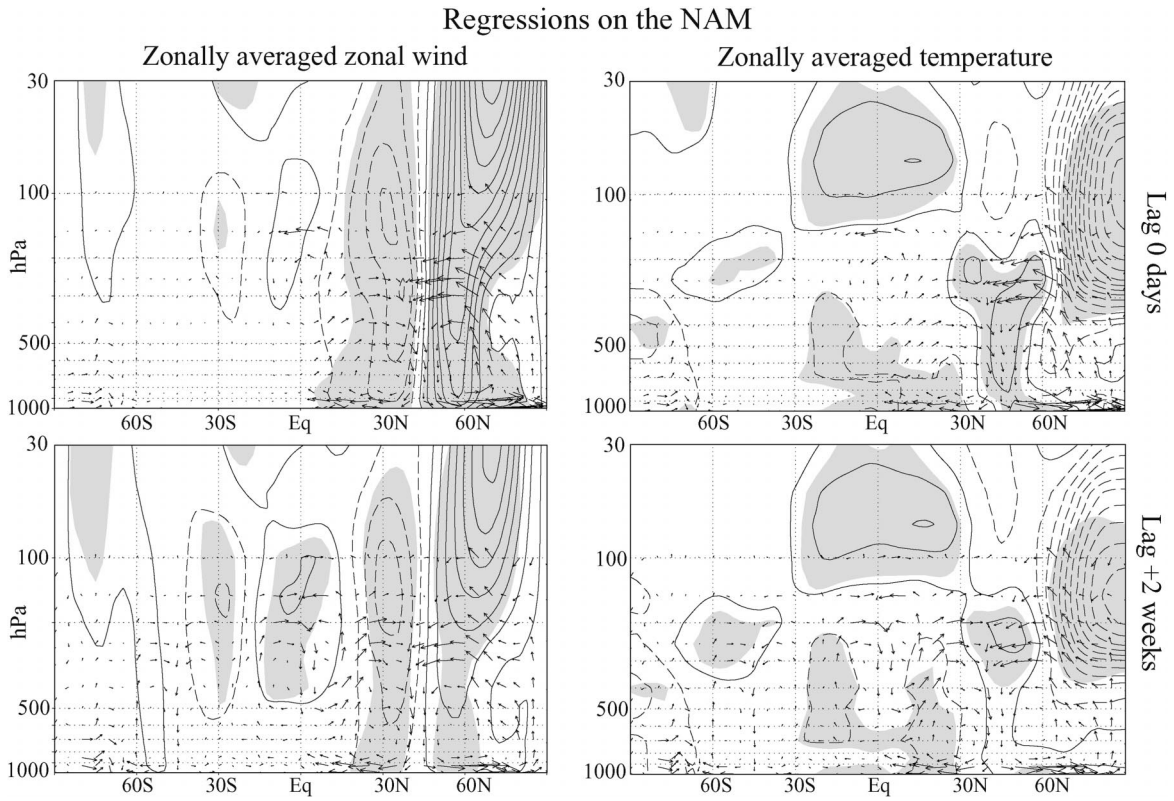

FIG. 1. (top left) Zonally averaged zonal wind (contours) and mean meridional circulation (vectors) anomalies regressed onto contemporaneous daily values of the NAM index time series centered on Jan–Mar. (top right) As in the left panel but contours are for zonally averaged temperature. (bottom) As in the top panels but the data are lagged by 2 weeks with respect to the NAM index time series. Contour intervals are 0.5 m s^{-1} (-0.75, -0.25, 0.25) for zonal wind and 0.2 K (-0.3, -0.1, 0.1) for temperature. The longest vector corresponds to $\sim$0.3 m s^{-1} (meridional) and $\sim$0.15 cm s^{-1} (vertical). Shading indicates correlations that exceed the 95% confidence level based on the *t* statistic. Negative contours are dashed.

robust during the Northern Hemisphere (NH) cold season, and were not found to be statistically significant during the NH warm season.

The section is divided into three parts: section 3a documents the global signature of the NAM in the zonally averaged tropospheric circulation; section 3b offers a physical interpretation of the results; and section 3c demonstrates that the amplitude of the NAM in the tropical troposphere is a function of the phase of the ENSO cycle. Note that since the analyses are linear, we describe the results in terms of the high index polarity only.

a. Observed linkages

The top panels in Fig. 1 show zonally averaged zonal wind (top left, contours), temperature (top-right, contours), and meridional circulation anomalies (top left and top right, vectors) regressed on contemporaneous daily JFM values of the NAM index time series for the global domain, 90°S–90°N, 1000–30-hPa. The extratropical features in the top panels in Fig. 1 are documented in previous studies (e.g., Thompson and Wallace 2000). The high index polarity of the NAM is associated with westerly anomalies along $\sim$55°N that extend and amplify with height into the lower stratosphere juxtaposed against tropospherically confined easterly anomalies along $\sim$30°N (Fig. 1, top left); cool anomalies over the polar cap juxtaposed against warm anomalies in the troposphere along $\sim$45°N; and counterclockwise-rotating meridional circulation anomalies between subpolar and midlatitudes juxtaposed against clockwise-rotating meridional circulation anomalies between subtropical and midlatitudes. As noted in Thompson and Wallace (2000), the sinking motion along 45°N coincides with regions of positive tropospheric temperature anomalies and the rising motion poleward of $\sim$60°N coincides with regions of negative temperature anomalies.

The most pronounced features observed in the top panels in Fig. 1 are found at NH extratropical latitudes, but two robust features are also evident at tropical latitudes: the high index polarity of the NAM is associated with statistically significant warm anomalies throughout the lower tropical stratosphere, and with statistically significant cool anomalies in the lower tropical troposphere that extend into the Southern Hemisphere (SH) subtropics. In this study, we focus on the structure, evolution, and dynamics of the signature of the NAM in the tropical troposphere. The relationship between the

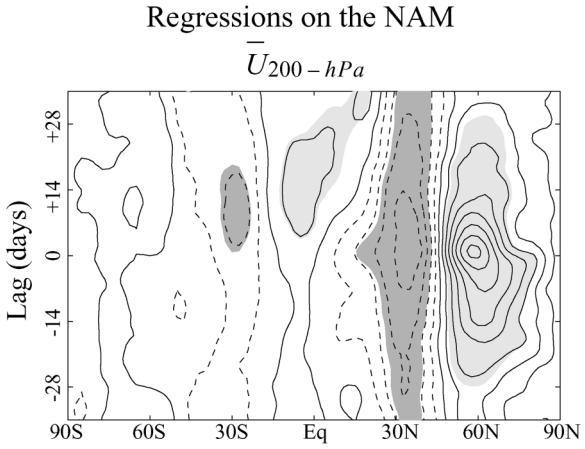

FIG. 2. Zonally averaged zonal wind anomalies at 200 hPa regressed onto standardized daily values of the NAM index time series for lags indicated. Positive lags indicate the zonal flow lags the NAM index time series, and vice versa. Contour intervals are 0.4 m s^{-1} (-0.2, 0.2, 0.6). Shading indicates correlations that exceed the 95% confidence level based on the *t* statistic. Negative contours are dashed.

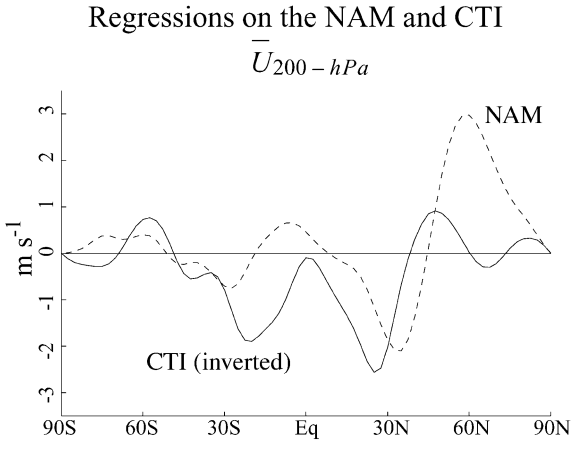

FIG. 3. Monthly mean, zonally averaged, zonal wind anomalies at 200 hPa regressed onto standardized values of the NAM index time series (dashed) and the inverted CTI time series (solid) during JFM 1979–99. The CTI time series is inverted such that positive values correspond to anomalously low sea surface temperature in the eastern tropical Pacific, and vice versa.

NAM and tropical stratospheric temperatures is discussed in Thompson and Wallace (2000) and is not examined here.

The temporal evolution of the NAM in the tropospheric zonal wind is examined in Fig. 2. The figure shows daily mean, zonally averaged zonal wind anomalies at 200 hPa regressed onto daily values of the NAM index time series for lags ranging from -35 to $+35$ days (note that the regression coefficients at lag 0 in Fig. 2 correspond to the regression coefficients at the 200-hPa level in the top-left panel in Fig. 1). The results in Fig. 2 reveal three key aspects of the NAM. First, they reveal the contrasting persistence of the extratropical centers of action of the NAM in the zonal wind: anomalies in the equatorward center of action tend to persist longer than anomalies in the poleward center of action. The enhanced persistence of the zonal wind anomalies in the equatorward center of action is consistent with the observation that the ENSO phenomenon projects onto the structure of the NAM in the zonal wind at subtropical latitudes but not at midlatitudes [Fig. 3; see also Robinson (2002) and Seager et al. (2003)]. The temporal correlations between indices of ENSO and the NAM are not statistically significant at any lag (not shown). But as discussed in Quadrelli and Wallace (2002) and later in this section, variations in the ENSO cycle are associated with substantial changes in the spatial structure of the NAM.

The second aspect of the NAM revealed in Fig. 2 is the poleward propagation of the zonal wind anomalies throughout the regression period, particularly at subtropical latitudes. The poleward migration of the zonal wind anomalies is reminiscent of findings reported in Feldstein (1998) and is consistent with the impact of the sphericity of earth on the direction of the propagation of wave activity away from the latitude of maximum zonal wind (Robinson 2000).

The third aspect of the NAM revealed in Fig. 2, and the aspect that is the focus of this paper, is the development of statistically significant zonal wind anomalies along the equator that start around day 0 and peak ~2–3 weeks following the peak in the NAM index time series. The equatorial westerly anomalies start in a narrow band about the equator at ~day 0, spread into a broad band about the equator by ~week 2, and then propagate into the NH subtropics by ~week 3. The region of significant correlations tracks the westerly anomalies as they grow and migrate northward. The high index polarity of the NAM is also associated with weak easterly anomalies in the SH subtropics that propagate southward, but the amplitude of this feature is comparatively weak. The tropical wind anomalies in Fig. 2 are clearly evident in results based on daily data with the seasonal mean removed (not shown), and thus do not reflect contamination of the NAM index time series by variations in ENSO.

From the results in Fig. 2, it follows that the tropical tropospheric features that are only weakly evident in the contemporaneous regressions in the top panels in Fig. 1 are more clearly evident when the data lag the NAM index time series by ~2 weeks (Fig. 1, bottom panels). At this time, the NAM resembles a banded structure in the anomalous tropospheric zonal wind field that extends from the polar regions of the NH deep into the subtropics of the SH. At tropical latitudes, the high index polarity of the NAM is characterized by equatorially symmetric westerly anomalies that extend throughout the upper tropical troposphere, off-equatorial cooling maxima that extend throughout the free troposphere at ~15°–20° latitude in both hemispheres, and paired tropospheric mean meridional circulation anomalies with

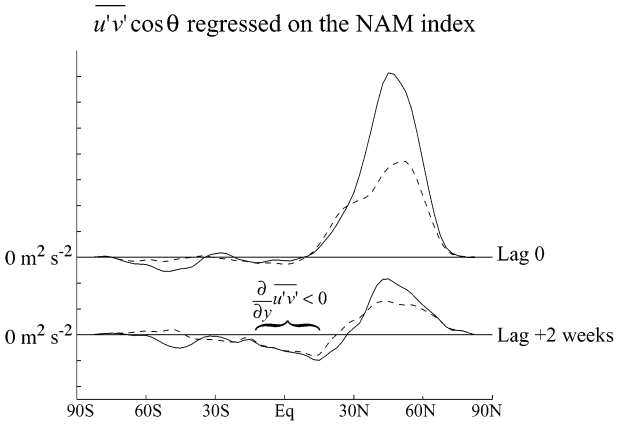

FIG. 4. Zonally averaged eddy momentum flux anomalies averaged over 300–100 hPa and regressed onto standardized daily values of the NAM index time series centered during JFM at lags indicated. Solid lines denote momentum flux anomalies by all eddies; dashed lines denote momentum flux anomalies by eddies with time scales longer than 10 days. Vertical tickmarks are at 2 m^2 s^{-2}.

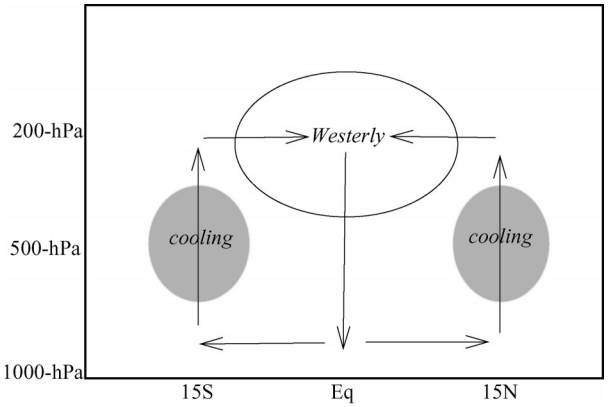

FIG. 5. Schematic of the response of the zonally averaged tropical tropospheric circulation to imposed westerly forcing (e.g., anomalous convergence of the zonally averaged eddy momentum flux) centered at ~200 hPa at the equator.

sinking motion near the equator and rising motion ~15°N and ~15°S.

b. Physical interpretation

What physical processes give rise to the tropical tropospheric anomalies observed in Figs. 1 and 2? In this section we hypothesize that the signature of the NAM in the tropical troposphere is consistent with waves interacting with the upper-tropospheric zonal flow over the eastern tropical Pacific. We first examine the dynamics of the linkages in the zonally averaged circulation.

The solid lines in Fig. 4 show zonally averaged eddy momentum flux anomalies ($\overline{u'v'}$, where the overbar denotes the zonal average and primes denote departures from the zonal average) averaged over 100–300 hPa and regressed onto the NAM index time series at a lag of 0 and +2 weeks (fluxes lagging). Note that the eddy momentum flux anomalies are multiplied by the cosine of latitude so that the results are proportional to wave activity (e.g., Edmon et al. 1980). In the contemporaneous regressions (Fig. 4, top), the high index polarity of the NAM is marked by anomalous poleward eddy momentum fluxes that extend from ~15° to 70°N. The associated regions of anomalous eddy momentum flux divergence and convergence reflect the *forcing* of the extratropical zonal flow by the eddies (e.g., Limpasuvan and Hartmann 1999, 2000; Lorenz and Hartmann 2003). At a lag of 2 weeks (Fig. 4, bottom), the anomalous eddy momentum fluxes not only act to reinforce the extratropical zonal wind anomalies (consistent with Lorenz and Hartmann 2003), but also to perturb the zonally averaged circulation throughout the Tropics. Two weeks after peak amplitude in the NAM, the entire upper tropical troposphere is marked by anomalous convergence of the eddy momentum flux. In contrast to the contemporaneous regressions, the lagged regressions can be interpreted as the *response* of the eddies to anomalies in the extratropical zonal flow (e.g., Lorenz and Hartmann 2003).

The dashed lines in Fig. 4 show the components of the eddy momentum flux anomalies that are due to the low-frequency eddies, where low frequency is defined as variability on time scales longer than 10 days. The anomalous fluxes due to low-frequency eddies were found by applying a 10-day low-pass Lanczos filter to the eddy components of the zonal and meridional wind fields before computing the associated covariances. In the deep Tropics, the low-frequency eddies account for virtually all of the eddy momentum flux anomalies observed 2 weeks after the peak in the NAM index time series (Fig. 4, bottom). In the extratropics, the low-frequency eddies account for roughly half of the total fluxes, consistent with findings reported in Limpasuvan and Hartmann (2000) and Lorenz and Hartmann (2003).

The anomalous eddy momentum flux convergence at tropical latitudes (Fig. 4, bottom) may be interpreted as driving the tropical signature evident in the bottom panels in Fig. 1. For example, consider the transient response of the tropical circulation to a westerly force applied at upper-tropospheric levels (Fig. 5). When the forcing is applied, the zonally averaged zonal wind accelerates toward the east throughout the forcing region. Away from the equator, the Coriolis force acting on the enhanced zonal flow drives equatorward motion in the upper troposphere that converges in the deep Tropics. The convergent meridional motion gives rise to sinking motion in the midtroposphere centered about the equator, but rising motion in the midtroposphere at subtropical latitudes (see also Haynes et al. 1991). Hence, both the equatorial westerly zonal wind anomalies and the paired tropical mean meridional circulation anomalies evident in the bottom panels in Fig. 1 are consistent with forcing by the anomalous eddy momentum flux convergence in the upper tropical troposphere.

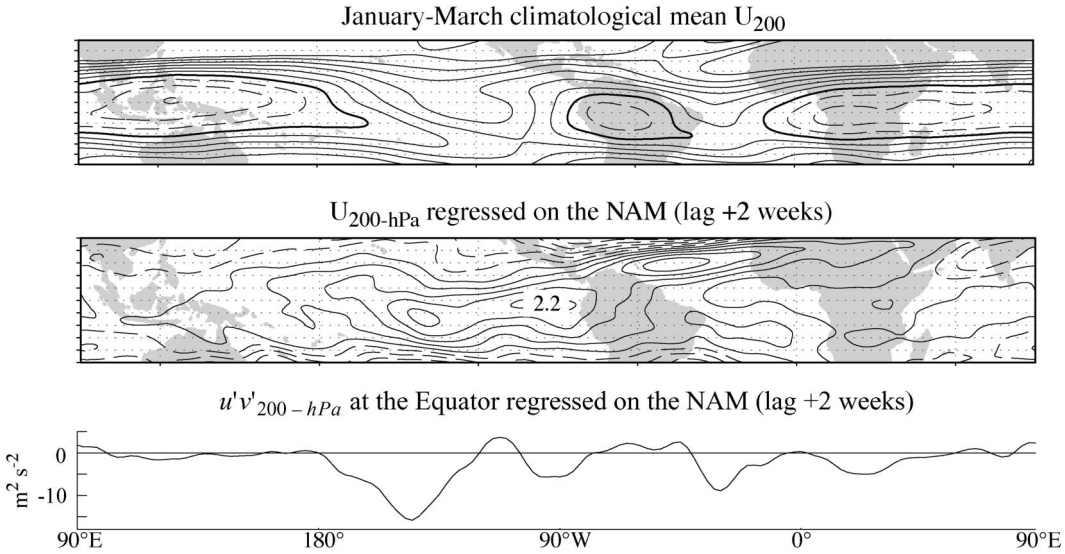

FIG. 6. (top) JFM climatological mean values of the zonal wind at 200 hPa; (middle) 200-hPa zonal wind anomalies regressed onto standardized daily values of the NAM index time series at a lag of 2 weeks (wind data lags the NAM); (bottom) cross-equatorial eddy momentum flux anomalies at 200 hPa regressed onto standardized daily values of the NAM index time series at a lag of 2 weeks (momentum flux lags the NAM). Contour intervals are (top) 5 m s^{-1} (-5, 0, 10 m s^{-1}) and (middle) 0.5 m s^{-1} (-0.75, -0.25, 0.25). (bottom) Tickmarks are spaced at 5 $m^2\ s^{-2}$. The zero contour is thickened. Negative contours are dashed.

The subtropical tropospheric temperature anomalies observed in the lower-right panel in Fig. 1 are also consistent with mechanical forcing centered about the equator. The cool anomalies in the subtropical troposphere are coincident with anomalous rising motion there, indicative of adiabatic changes in temperature. Similarly, the anomalous vertical shear of the zonal flow along 30°S is consistent with the induced weakening of the meridional temperature gradient south of 15°S. The anomalous sinking motion at the equator does not overlie a band of anomalous warming, presumably because the lapse rate of the deep Tropics is strongly constrained by diabatic forcing. To what extent the positive polarity of the NAM suppresses diabatic heating in the Tropics remains to be determined.

Why is the NAM associated with anomalies in the eddy momentum flux convergence at tropical latitudes? Observations and theory suggest that extratropical eddies disturb the tropical troposphere in the vicinity of the Pacific westerly duct, a broad band of upper-tropospheric westerlies that overlies the eastern tropical Pacific primarily during the NH cold season (e.g., Webster and Holton 1982; Kiladis and Wieckmann 1992, 1997; Hoskins and Ambrizzi 1993; Tomas and Webster 1994). For low frequency Rossby waves in which the zonal wavenumber is much smaller than the stationary wavenumber, the meridional group velocity of the wave decreases as the zonal wind decreases (e.g., Hoskins and Karoly 1981; Webster and Holton 1982). Thus, it follows that the amplitude of extratropical wave activity in the westerly duct is partially determined by the strength of the subtropical zonal flow: when the subtropical zonal flow is weaker than normal, dissipation has more time to damp disturbances before they reach tropical latitudes, and vice versa. Based on this reasoning, the high index phase of the NAM should not only favor weaker-than-normal zonal flow at subtropical latitudes (Fig. 1), but also decreased wave activity in the eastern tropical Pacific, and vice versa. Figure 6 suggests that this is, in fact, the case.

The top panel in Fig. 6 shows the JFM climatological mean zonal wind at 200 hPa between 30°S and 30°N, the middle panel shows 200-hPa zonal wind anomalies between 30°S and 30°N, and the bottom panel shows 200-hPa cross-equatorial eddy momentum flux anomalies regressed onto daily values of the NAM index time series at a lag of 2 weeks. Consistent with the discussion in the previous paragraph, the high index polarity of the NAM is associated with enhanced westerly wind and southward eddy momentum flux anomalies throughout the eastern tropical Pacific (middle and bottom panels), coincident with the broad band of climatological westerlies there (top panel). The southward eddy momentum flux anomalies are indicative of a decrease in southward-propagating eddy activity. Weak zonal wind and momentum flux anomalies are also observed over the equatorial Atlantic, coincident with the relatively narrow band of climatological westerlies there.

Together, the evidence presented in this section suggests that the signature of the NAM in the tropical troposphere reflects the impact of the NAM on the propagation of wave activity into the westerly duct over the eastern tropical Pacific. In the next section, we dem-

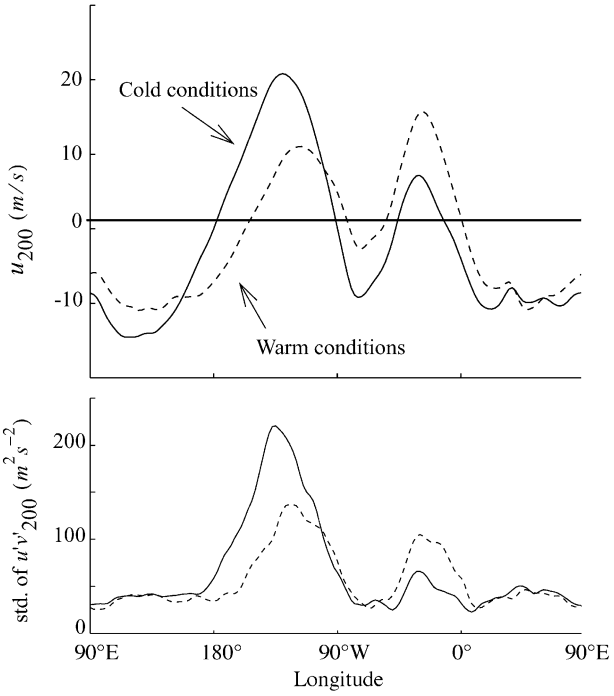

FIG. 7. JFM values of (top) the climatological mean zonal wind and (bottom) the climatological std dev of the eddy momentum flux at 200 hPa along the equator. Results are shown for terciles of the data corresponding to the cold (solid) and warm (dashed) phases of the ENSO cycle. The years used in the analysis are listed in Table 1.

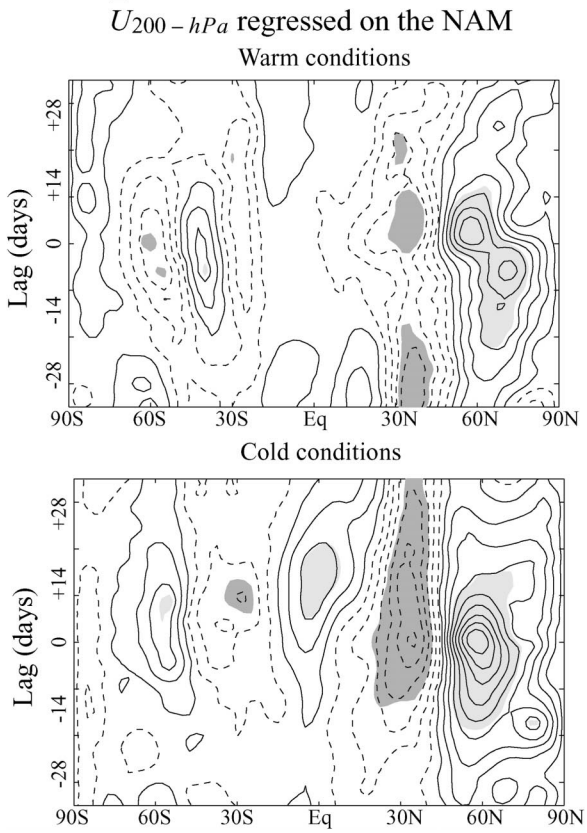

FIG. 8. As in Fig. 2, but for terciles of the data corresponding to the (top) warm and (bottom) cold phases of the ENSO cycle. The years used in the analysis are listed in Table 1.

onstrate that these linkages are a function of the phase of the ENSO cycle.

c. Relationship with ENSO

In the previous section, we argued that the amplitude of extratropical wave activity in the eastern tropical Pacific is partially determined by the strength of the subtropical zonal flow. As noted in Webster and Holton (1982), the amplitude of wave activity in the eastern tropical Pacific is also a function of the strength of the local westerlies: when the flow in the westerly duct is anomalous westerly, disturbances have a larger meridional group velocity and can propagate farther before they are damped, and vice versa. Thus, changes in tropical SSTs associated with the ENSO phenomenon not only impact the magnitude of the westerlies in the eastern tropical Pacific, but also the amount of wave activity there: the cold phase of the ENSO cycle is characterized by a relatively broad band of equatorial westerlies and enhanced variance of the eddy momentum flux in the eastern tropical Pacific; the warm phase of the ENSO cycle is characterized by anomalies in the opposite sense (Fig. 7; Kiladis 1998; Matthews and Kiladis 1999; Waugh and Polvani 2000). On the basis of the hypothesis outlined in the previous section, winters corresponding to the cold phase of the ENSO cycle should also favor an enhanced linkage between the NAM and the tropical circulation.

Figures 8 and 9 show results analogous to those presented in Fig. 1 (bottom left) and Fig. 2, but for terciles of the data corresponding to (top panels) warm and (bottom panels) cold conditions in the eastern tropical Pacific. The terciles used in the analysis are defined on the basis of the CTI time series (as defined in section 2) and are listed in Table 1. Statistical significance is assessed assuming one-third the number of degrees of freedom used in the previous section. As evidenced in both figures, the linkages between the NAM and the circulation of the tropical troposphere are, in fact, more robust during the cold phase of ENSO. During cold ENSO winters, the NAM is associated with equatorial westerlies that develop ~1–2 weeks following the peak in the NAM index time series (Fig. 8, bottom), and at a lag of 2 weeks, with a pattern of tropical climate anomalies reminiscent of the results presented in the previous section (Fig. 9, bottom). During warm ENSO winters the NAM is not significantly related to variations in the tropical circulation at any lag (Figs. 8 and 9, top).

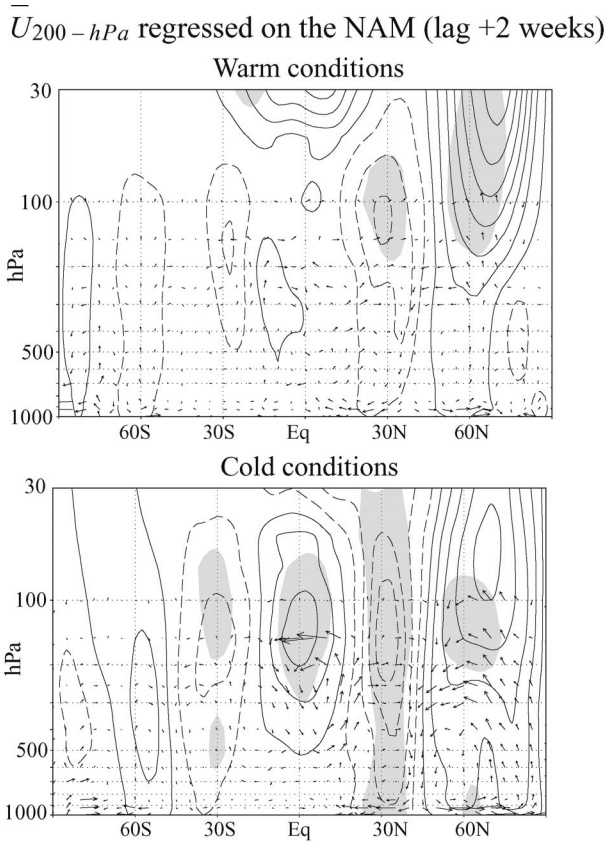

FIG. 9. As in the bottom-left panel in Fig. 1, but for terciles of the data corresponding to the (top) warm and (bottom) cold phases of the ENSO cycle. The years used in the analysis are listed in Table 1. Circulation anomalies lag the NAM by 2 weeks.

4. The signature of the SAM in the tropical troposphere

In this section, we provide a companion analysis for the relationship between the SAM and the circulation of the tropical troposphere. As is the case for the NAM, results for the SAM are most robust during the associated cold season. Results for the SH warm season were not found to be statistically significant at any lag.

Figure 10 shows lag regressions between zonal wind anomalies at 200 hPa and daily values of the SAM index time series for lags ranging from −35 to +35 days centered on data for June–August (i.e., the figure is analogous to Fig. 2, but is based on the SAM index time series during SH winter). As noted in the introduction, the largest anomalies associated with the SAM are located at ~35° and ~60°S. In contrast to the NAM, the equatorward center of action of the SAM exhibits less persistence than the poleward center of action. The contrasting persistence of the equatorward centers of action of the NAM and SAM during the respective winter seasons is consistent with the observation that the ENSO cycle typically peaks in amplitude during NH winter (e.g., Rasmusson and Carpenter 1982; Wallace et al. 1998). Like the NAM, the high index polarity of the SAM is associated with westerly wind anomalies in the upper tropical troposphere that peak roughly ~1–2 weeks after the peak in the SAM index time series and migrate southward as they decay. The coupling between the SAM and the tropical tropospheric zonal flow is weaker than that observed in association with the NAM, but is nevertheless statistically significant.

TABLE 1. Terciles used in Figs. 8 and 9. Terciles are for winter seasons (JFM 1979–99) corresponding to warm and cold conditions in the eastern tropical Pacific. Warm and cold conditions are defined on the basis of sea surface temperature anomalies averaged between 6°N–6°S; and 180°–90°W.

Phase of ENSO	Years
Warm	1983, 1987, 1988, 1992, 1993, 1995, 1998
Cold	1981, 1985, 1986, 1989, 1994, 1996, 1999

Figure 11 shows zonally averaged zonal wind, temperature, and meridional circulation anomalies regressed on daily values of the SAM index time series for (top panel) lags of zero and (bottom panel) 2 weeks. As is the case with the NAM, the high index polarity of the SAM is followed by anomalous westerlies in the upper tropical troposphere and paired meridional circulation anomalies with sinking motion at the equator and rising motion at subtropical latitudes (Fig. 11, bottom). The corresponding regression coefficients for tropical temperature anomalies are not statistically significant, and do not exceed the contour threshold. Like the NAM, the tropical upper-tropospheric zonal wind anomalies observed in association with the SAM coincide with anomalies in the momentum flux convergence by low-frequency eddies at tropical latitudes (Fig. 12, bottom; note that the results are inverted such that positive values denote southward eddy momentum flux anomalies, and vice versa). Also like the NAM, the largest tropical westerly wind anomalies and cross-equatorial eddy momentum flux anomalies observed 2 weeks following

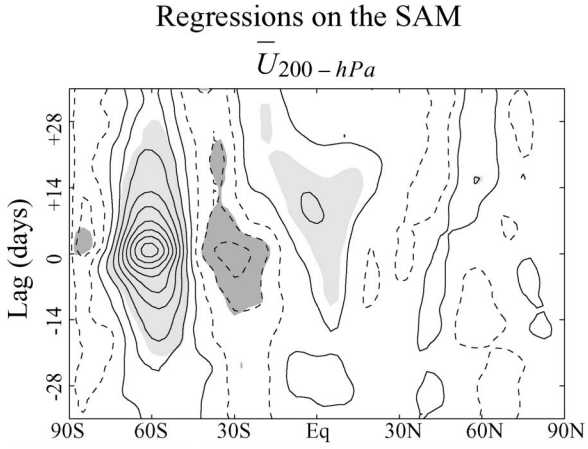

FIG. 10. As in Fig. 2, but for regressions based on daily values of the SAM index time series centered on Jun–Aug.

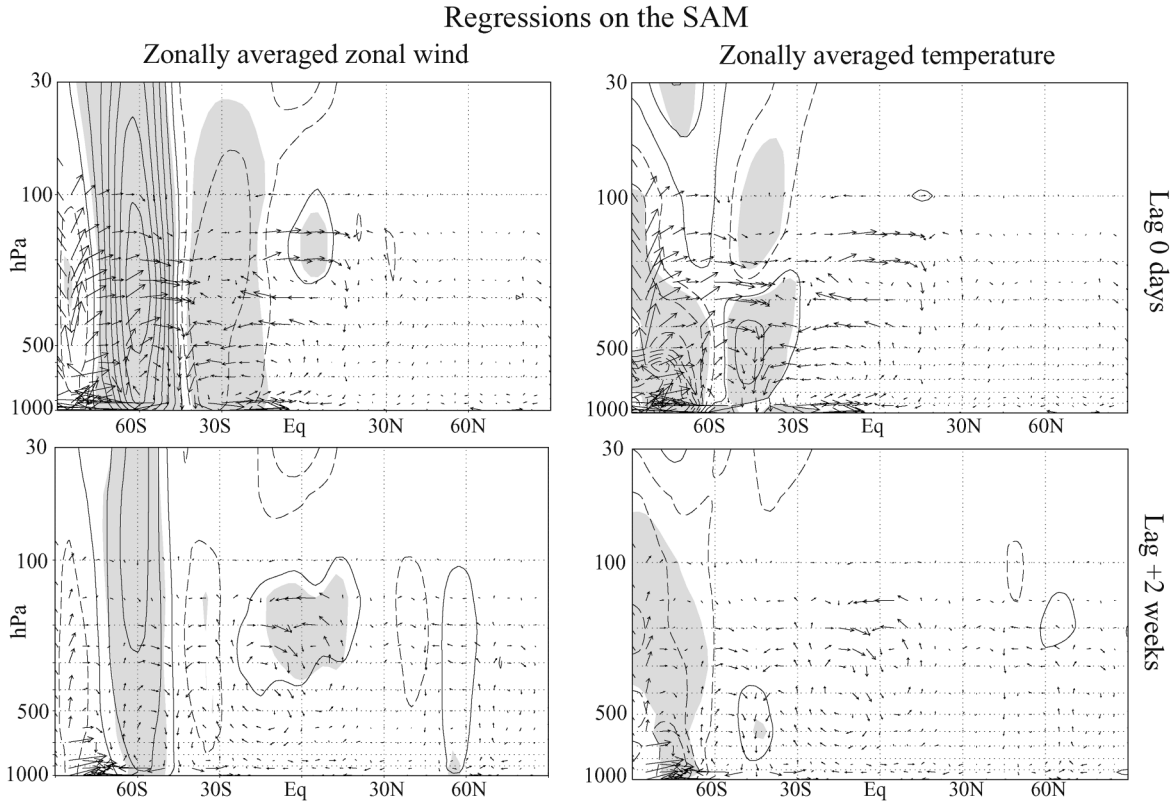

FIG. 11. As in Fig. 1, but for regressions based on daily values of the SAM index time series centered on Jun–Aug.

peak amplitude in the SAM are located over the eastern tropical Pacific (Fig. 13, middle and bottom panels). In contrast to the NAM, the tropical signature of the SAM does not exhibit a robust dependence on the phase of the ENSO cycle (not shown).

The results in Figs. 10–13 suggest that the SAM is coupled to the circulation of the Tropics in a manner analogous to that observed in association with the NAM, but with substantially weaker amplitude. The weaker amplitude of the tropical signature of the SAM is consistent with the absence of a pronounced westerly duct during the SH cold season (Fig. 13, top), conditions which act to suppress the propagation of wave activity into tropical latitudes (Webster and Holton 1982).

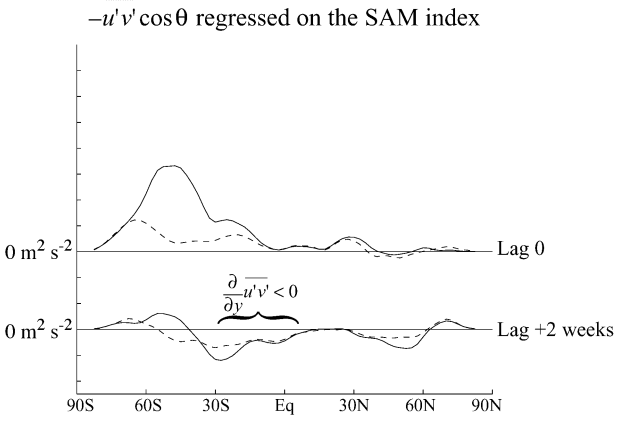

FIG. 12. As in Fig. 4, but for regressions based on daily values of the SAM index time series centered on Jun–Aug. Results are inverted such that positive values denoted southward eddy momentum flux anomalies, and vice versa.

5. Summary and concluding remarks

The findings reported in this study suggest that the annular modes should be viewed not as patterns of variability restricted to their respective hemispheres, but as structures that extend deep into the Tropics and subtropics of the opposing hemisphere. In the tropical troposphere, the high index polarity of the annular modes is associated with westerly anomalies centered about the equator at ~200 hPa flanked by cool anomalies that peak in the subtropical troposphere of both hemispheres. The tropical signature of the annular modes is observed in association with both annular modes during their respective winter seasons, but has substantially larger amplitude in association with the NAM. The linkages between the annular modes and the circulation of the tropical troposphere are most robust when the tropical circulation lags indices of the annular modes by ~2 weeks. Variations in the extratropical annular modes may thus prove useful for predicting certain aspects of tropical climate variability.

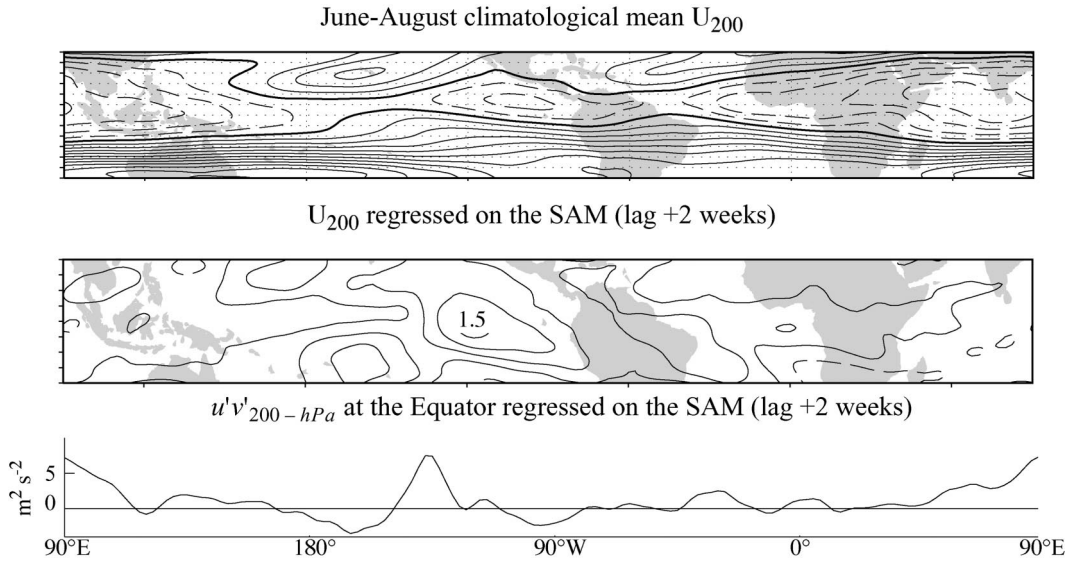

FIG. 13. As in Fig. 6, but for Jun–Aug data and regressions based on daily values of the SAM index time series.

The tropical features revealed in this study are consistent with momentum forcing by waves originating at extratropical latitudes. During the high index polarity of the annular modes, the zonal wind along ~30°–40° latitude is anomalously weak, conditions which favor greater dissipation of extratropical waves before they reach tropical latitudes. Hence, during the ~1–2-week period following peak amplitude in the extratropical annular modes, there is less wave breaking at tropical latitudes, and the upper tropical troposphere experiences anomalous westerly forcing.

The anomalous westerly forcing in the upper tropical troposphere drives westerly anomalies at the equator and hemispherically symmetric mean meridional circulation anomalies, with anomalous sinking motion near the equator and anomalous rising motion in the subtropics of both hemispheres. The anomalous rising motion in the subtropics overlies regions of anomalous cooling, indicative of adiabatically induced changes in temperature. The anomalous sinking motion near the equator does not overlie an analogous region of anomalous warming, presumably because the lapse rate in the deep Tropics is strongly constrained by diabatic forcing. Hence, when averaged over the entire Tropics, the high index polarity of the NAM is associated with a net decrease in tropical tropospheric temperatures. During the NH winter, the high index polarity of the NAM is thus associated with anomalous cooling in the tropical troposphere juxtaposed against anomalous warming in the tropical lower stratosphere (Thompson and Wallace 2000).

The relationships between the annular modes and the zonal flow of the Tropics are most pronounced in the vicinity of the westerly duct in the eastern tropical Pacific, consistent with the hypothesis that the tropical tropospheric signature of the annular modes reflects interactions between equatorward-propagating waves and the tropical zonal flow. The linkages between the NAM and the tropical troposphere are more robust than those observed in association with the SAM, presumably because the westerly duct is most robust during the NH cold season.

The amplitude of the relationship between the NAM and the tropical circulation is a function of the phase of the ENSO cycle: the cold phase of the ENSO cycle is associated with an enhanced linkage between the NAM and the tropical circulation, and vice versa. We argued that this finding is consistent with the impact of ENSO on the amplitude of the westerlies and wave activity in the eastern tropical Pacific (Kiladis 1998; Matthews and Kiladis 1999; Waugh and Polvani 2000). But it is notable that this finding is also consistent with the enhanced variance of the NAM over the North Pacific sector during cold ENSO winters (Quadrelli and Wallace 2002). The linkage between the SAM and the tropical troposphere does not exhibit an analogous relationship with the phase of the ENSO cycle.

The signature of the annular modes in tropical sea level pressures observed in Baldwin (2001) differs from the relationships revealed in this study in the following respects: 1) the correlations between the annular modes and tropical sea level pressures peak at zero lag, whereas the linkages observed in this study peak at a lag of ~2 weeks (cf. this study's Fig. 2 and Baldwin's 2001 Fig. 3); and 2) the contemporaneous profile of the annular modes in SLP is asymmetric about the equator, whereas the lagged signature revealed in this study exhibits a high level of equatorial symmetry. Hence, the near-instantaneous signature of the annular modes in tropical sea level pressures discussed in Baldwin (2001) likely reflects a fundamentally different physical relationship than that revealed here.

Correlations between daily indices of the NAM and the SAM were not found to be statistically significant at any lag, despite the fact that both annular modes perturb the circulation of the Tropics in an analogous manner (see also Baldwin 2001). The absence of significant correlations between time indices of the NAM and the SAM is consistent with our finding that the annular modes perturb the Tropics during different times of year, and our hypothesis that the tropical signature of the annular modes reflects the response of the tropical circulation to variations in extratropical wave activity.

At least two observations suggest that the signature revealed in this study reflects a preferred response of the tropical circulation to anomalous mechanical forcing. First, the tropical signature of the annular modes exhibits a remarkable degree of equatorial symmetry, despite the fact there is no physical reason to expect the associated anomalies in the eddy momentum flux convergence to be similarly symmetric. Second, the tropical signature of the NAM emerges as a dominant pattern of variability in its own right based on empirical orthogonal function (EOF) analysis of the tropospheric circulation. Dima (2002) recovered a similar structure as the second EOF of 200-hPa streamfunction anomalies during the NH winter season (the first EOF corresponds to ENSO) and Watanabe et al. (2002) recovered a similar pattern as the leading EOF of ENSO-residual 300-hPa streamfunction anomalies for all months of the year. Figure 14 demonstrates that the tropical tropospheric signature of the annular modes also emerges as the leading EOF of both the zonally varying and the zonally averaged tropical tropospheric ENSO-residual zonal wind field during NH winter. The tropical tropospheric ENSO-residual zonal wind data ($U_{\text{ENSO-residual}}$) was generated by regressing the CTI time series from the monthly mean zonal wind at all grid points 1000–100 hPa and 40°S–40°N. As evidenced in Fig. 14, the patterns derived by regressing the anomalous zonally averaged circulation onto the leading PC time series of $U_{\text{ENSO-residual}}$ and $\overline{U}_{\text{ENSO-residual}}$ strongly resemble the global signature of the NAM revealed in this paper. The corresponding PC time series account for 14% and 34% of the total ENSO-residual variance in the anomalous zonally varying and zonally averaged tropical tropospheric zonal wind fields, respectively.

The NAM and the SAM have both exhibited trends toward their high index polarity over the past few decades, which have made substantial contributions to observed climate change in the extratropics of their respective hemispheres (e.g., Hurrell 1995; Thompson et al. 2000; Thompson and Solomon 2002). The results in this paper imply that the recent trends in the annular modes are also reflected in observed climate change at tropical latitudes. The contribution of the annular modes to trends in the Tropics was examined using contemporaneous monthly mean values of the NAM index time series, tropical mean (30°N–30°S) Microwave Sounding Unit channel 2LT (MSU2LT) temperatures (which are indicative of tropospheric temperatures centered at

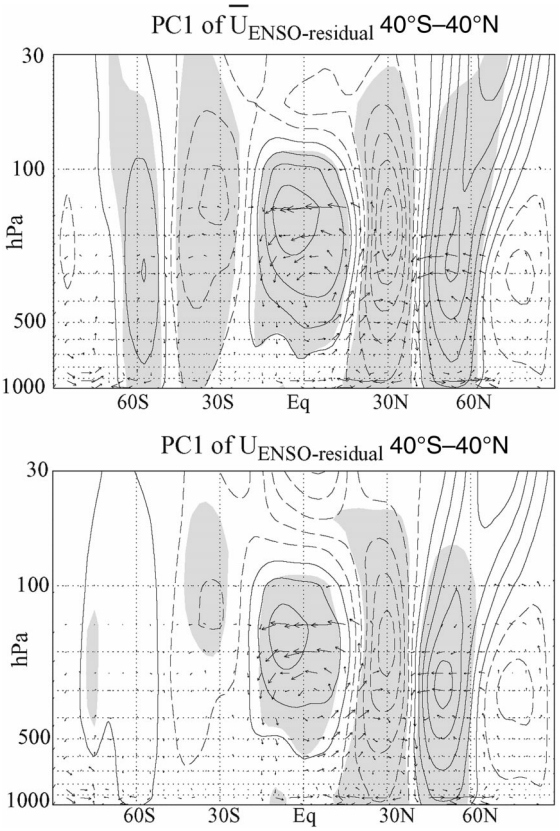

FIG. 14. Zonally averaged zonal wind (contours) and mean meridional circulation (vectors) anomalies regressed onto (top) the leading PC time series of the ENSO-residual zonally averaged zonal wind at 1000–100 hPa and 40°S–40°N and (bottom) the leading PC time series of ENSO-residual zonal wind anomalies at 1000–100-hPa and 40°S–40°N. Contour intervals are 0.5 m s^{-1} (−0.75, −0.25, 0.25) for zonal wind. The longest vector corresponds to ~0.3 m s^{-1} (meridional) and ~0.15 cm s^{-1} (vertical). Shading denotes correlations that exceed the 95% confidence level based on the *t* statistic. Negative contours are dashed. The ENSO-residual data are formed by linearly regressing the CTI time series from the data at each grid point.

~600 hPa) and tropical mean surface temperatures by applying the methodology outlined in Thompson et al. (2000). The results are summarized in Table 2. During the NH winter months when the trend in the NAM is

TABLE 2. (first and third rows) The 20-yr (1979–99) linear trends in tropical mean (30°N–30°S) surface air temperatures (SAT), MSU2LT temperatures, and lower tropospheric static stability (defined as MSU2LT minus SAT) for seasons indicated [K (20 yr)$^{-1}$]. (second and fourth rows) The components of the trends that are linearly congruent with month-to-month variations in the NAM index time series.

	$SAT_{30°N–30°S}$	$MSU2LT_{30°N–30°S}$	$MSU2LT_{30°N–30°S} - SAT_{30°N–30°S}$
JFM trend	0.29	−0.07	−0.36
Congruent with NAM	−0.05	−0.10	−0.05
Annual mean trend	0.29	−0.01	−0.30
Congruent with NAM	−0.01	−0.02	−0.01

largest (Thompson et al. 2000), variations in the NAM are linearly congruent with a −0.10-K decrease in tropical mean MSU2LT temperatures between 1979 and 1999 (Table 2, second column) but with a relatively small change in tropical mean surface temperatures (−0.05 K; Table 2, first column). As such, the recent trend in the NAM has contributed to ~15% of the discrepancy between temperature trends at the surface and the free troposphere in the Tropics during the NH winter months [Table 2; third column; see the National Research Council Panel on Reconciling Temperature Observations (2000) for a synopsis of the discrepancy between temperature trends at the surface and in the free troposphere). However, the trend in the NAM accounts for a negligible fraction of tropical mean trends in lower-tropospheric static stability in data for all months of the year (Table 2; bottom row of third column), in accord with findings reported in Hegerl and Wallace (2002). The recent trend in the SAM has not noticeably contributed to trends in tropical mean temperatures (not shown).

Acknowledgments. We thank B. J. Hoskins and J. M. Wallace for helpful discussions during the formative stages of this research, and two anonymous reviewers for useful comments on the manuscript. DWJT was supported by National Science Foundation Grants CAREER: ATM-0132190 and ATM-0320959 from the Climate Dynamics Program. DJL was supported by National Science Foundation Grant ATM-9873691 from the Climate Dynamics Program.

REFERENCES

Baldwin, M. P., 2001: Annular modes in global daily surface pressure. *Geophys. Res. Lett.,* **28,** 4115–4118.

Bretherton, C. S., M. Widmann, V. P. Dymnikov, J. M. Wallace, and I. Blad, 1999: The effective number of spatial degrees of freedom of a time-varying field. *J. Climate,* **12,** 1990–2009.

Czaja, A., P. van der Vaart, and J. Marshall, 2002: A diagnostic study of the role of remote forcing in tropical Atlantic variability. *J. Climate,* **15,** 3280–3290.

Dima, I., 2002: Annular structures in low latitude wind and temperature variability. M.S. Thesis, Department of Atmospheric Sciences, University of Washington, 127 pp. [Available from the University of Washington Libraries, Box 352900, Seattle, WA 98195-2900.]

Edmon, H. J., B. J. Hoskins, and M. E. McIntyre, 1980: Eliassen–Palm cross sections for the troposphere. *J. Atmos. Sci.,* **37,** 2600–2616.

Feldstein, S. B., 1998: An observational study of the intraseasonal poleward propagation of zonal mean flow anomalies. *J. Atmos. Sci.,* **55,** 2516–2529.

Gong, D., and S. Wang, 1999: Definition of Antarctic Oscillation index. *Geophys. Res. Lett.,* **26,** 459–462.

Hartmann, D. L., and F. Lo, 1998: Wave-driven zonal flow vacillation in the Southern Hemisphere. *J. Atmos. Sci.,* **55,** 1303–1315.

Haynes, P. H., C. J. Marks, M. E. McIntyre, T. G. Shepherd, and K. P. Shine, 1991: On the downward control of extratropical diabatic circulations by eddy-induced mean zonal forces. *J. Atmos. Sci.,* **48,** 651–678.

Hegerl, G. C., and J. M. Wallace, 2002: Influence of patterns of climate variability on the difference between satellite and surface temperature trends. *J. Climate,* **15,** 2412–2428.

Hoskins, B. J., and D. J. Karoly, 1981: The steady linear response of a spherical atmosphere to thermal and orographic forcing. *J. Atmos. Sci.,* **38,** 1179–1196.

——, and T. Ambrizzi, 1993: Rossby wave propagation on a realistic longitudinally varying flow. *J. Atmos. Sci.,* **50,** 1661–1671.

Hurrell, J. W., 1995: Decadal trends in the North Atlantic Oscillation region temperatures and precipitation. *Science,* **269,** 676–679.

——, Y. Kushnir, G. Ottersen, and M. Visbeck, Eds., 2002: *The North Atlantic Oscillation: Climate Significance and Environmental Impact. Geophys. Monogr.,* No. 134, Amer. Geophys. Union, 279 pp.

Jones, P. D., 1994: Hemispheric surface air temperature variations: A reanalysis and update to 1993. *J. Climate,* **7,** 1794–1802.

Kalnay, E., and Coauthors, 1996: The NCEP/NCAR 40-Year Reanalysis Project. *Bull. Amer. Meteor. Soc.,* **77,** 437–471.

Karoly, D. J., 1990: The role of transient eddies in low-frequency zonal variations of the Southern Hemisphere circulation. *Tellus,* **42A,** 41–50.

Kidson, J. W., 1988a: Indices of the Southern Hemisphere zonal wind. *J. Climate,* **1,** 183–194.

——, 1988b: Interannual variations in the Southern Hemisphere circulation. *J. Climate,* **1,** 1177–1198.

Kiladis, G. N., 1998: Observations of Rossby waves linked to convection over the eastern tropical Pacific. *J. Atmos. Sci.,* **55,** 321–339.

——, and K. M. Weickmann, 1992: Extratropical forcing of tropical Pacific convection during northern winter. *Mon. Wea. Rev.,* **120,** 1924–1938.

——, and ——, 1997: Horizontal structure and seasonality of large-scale circulations associated with tropical convection. *Mon. Wea. Rev.,* **125,** 1997–2013.

Lamb, P. J., and R. A. Peppler, 1987: North Atlantic Oscillation: Concept and application. *Bull. Amer. Meteor. Soc.,* **68,** 1218–1225.

Limpasuvan, V., and D. L. Hartmann, 1999: Eddies and the annular modes of climate variability. *Geophys. Res. Lett.,* **26,** 3133–3136.

——, and ——, 2000: Wave-maintained annular modes of climate variability. *J. Climate,* **13,** 4414–4429.

Lorenz, D. J., and D. L. Hartmann, 2001: Eddy–zonal flow feedback in the Southern Hemisphere. *J. Atmos. Sci.,* **58,** 3312–3327.

——, and ——, 2003: Eddy–zonal flow feedback in the Northern Hemisphere. *J. Climate,* **16,** 1212–1227.

Malmgren, B. A., A. Winter, and D. Chen, 1998: El Niño–Southern Oscillation and North Atlantic Oscillation control of climate in Puerto Rico. *J. Climate,* **11,** 2713–2718.

Matthews, A. J., and G. N. Kiladis, 1999: Interactions between ENSO, transient circulation, and tropical convection over the Pacific. *J. Climate,* **12,** 3062–3086.

McHugh, M. J., and J. C. Rogers, 2001: North Atlantic Oscillation influence on precipitation variability around the Southeast African convergence zone. *J. Climate,* **14,** 3631–3642.

Meehl, G. A., and H. van Loon, 1979: The seesaw in winter temperatures between Greenland and Northern Europe. Part II: Teleconnections with lower latitudes. *Mon. Wea. Rev.,* **107,** 1095–1106.

Mo, K. C., and G. H. White, 1985: Teleconnections in the Southern Hemisphere. *Mon. Wea. Rev.,* **113,** 22–37.

Moulin, C., C. E. Lambert, F. Dulac, and U. Dayan, 1997: Control of atmospheric export of dust from North Africa by the North Atlantic Oscillation. *Nature,* **387,** 691–694.

National Research Council Panel on Reconciling Temperature Observations, 2000: *Reconciling Observations of Global Temperature Change.* National Academy Press, 104 pp.

Quadrelli, R., and J. M. Wallace, 2002: Dependence of the structure of the Northern Hemisphere annular mode on the polarity of ENSO. *Geophys. Res. Lett.,* **29,** 2132, doi:10.1029/2002GL015807.

Rasmusson, E., and T. Carpenter, 1982: Variations in the tropical sea

surface temperature and surface wind fields associated with the Southern Oscillation/El Niño. *Mon. Wea. Rev.,* **110,** 354–384.

Robinson, W. A., 2000: A baroclinic mechanism for the eddy feedback on the zonal index. *J. Atmos. Sci.,* **57,** 415–422.

——, 2002: On the midlatitude thermal response to tropical warmth. *Geophys. Res. Lett.,* **29,** 1190, doi:10.1029/2001GL014158.

Rogers, J. C., and H. van Loon, 1982: Spatial variability of sea level pressures and 500 mb height anomalies over the Southern Hemisphere. *Mon. Wea. Rev.,* **110,** 1375–1392.

Seager, R., N. Harnik, Y. Kushnir, W. Robinson, and J. A. Miller, 2003: Mechanisms of hemispherically symmetric climate variability. *J. Climate,* **16,** 2960–2978.

Shiotani, M., 1990: Low-frequency variations of the zonal mean state of the Southern Hemisphere troposphere. *J. Meteor. Soc. Japan,* **68,** 461–471.

Spencer, R. W., and J. R. Christy, 1992: Precision and radiosonde validation of satellite gridpoint temperature anomalies. Part II: A tropospheric retrieval and trends during 1979–90. *J. Climate,* **5,** 858–866.

Thompson, D. W. J., and J. M. Wallace, 1998: The Arctic Oscillation signature in the wintertime geopotential height and temperature fields. *Geophys. Res. Lett.,* **25,** 1297–1300.

——, and ——, 2000: Annular modes in the extratropical circulation. Part I: Month-to-month variability. *J. Climate,* **13,** 1000–1016.

——, and S. Solomon, 2002: Interpretation of recent Southern Hemisphere climate change. *Science,* **296,** 895–899.

——, J. M. Wallace, and G. C. Hegerl, 2000: Annular modes in the extratropical circulation. Part II: Trends. *J. Climate,* **13,** 1018–1036.

Tomas, R. A., and P. J. Webster, 1994: Horizontal and vertical structure of cross-equatorial wave propagation. *J. Atmos. Sci.,* **51,** 1417–1430.

van Loon, H., and J. Rogers, 1978: The seesaw in winter temperatures between Greenland and Northern Europe. Part I: General description. *Mon. Wea. Rev.,* **106,** 296–310.

Walker, G. T., and E. W. Bliss, 1932: World Weather V. *Mem. Roy. Meteor. Soc.,* **4,** 53–84.

Wallace, J. M., and D. S. Gutzler, 1981: Teleconnections in the geopotential height field during the Northern Hemisphere winter. *Mon. Wea. Rev.,* **109,** 784–812.

——, E. M. Rasmusson, T. P. Mitchell, V. E. Kousky, E. S. Sarachik, and H. von Storch, 1998: On the structure and evolution of ENSO-related climate variability in the tropical Pacific: Lessons from TOGA. *J. Geophys. Res.,* **103C,** 14 241–14 259.

Watanabe, M., F.-F. Jin, and M. Kimoto, 2002: Tropical axisymmetric mode of variability in the atmospheric circulation: Dynamics as a neutral mode. *J. Climate,* **15,** 1537–1554.

Waugh, D. W., and L. M. Polvani, 2000: Climatology of intrusions into the tropical upper troposphere. *Geophys. Res. Lett.,* **27,** 3857–3860.

Webster, P. J., and J. R. Holton, 1982: Cross-equatorial response to middle-latitude forcing with a latitudinally and zonally nonuniform basic state. *J. Atmos. Sci.,* **39,** 722–733.

Yoden, S., M. Shiotani, and I. Hirota, 1987: Multiple planetary flow regimes in the Southern Hemisphere. *J. Meteor. Soc. Japan,* **65,** 571–585.